Electronic Supplementary Material (ESI) for Nanoscale.
This journal is © The Royal Society of Chemistry 2014

SUPPLEMENTARY INFORMATION

Observation of the Origin of d^0 Magnetism in ZnO Nanostructures Using X-ray-based Microscopic and Spectroscopic Techniques

Shashi B. Singh *et al.*

Figure **S1** displays the valence-band DOSs at/below the valence-band maximum (E_{VBM}) or Fermi level (E_F) of ZnO NC and NW, which were obtained using spatially resolved SPEM with an incident photon energy of 380 eV. The zero energy is chosen to be at the E_{VBM} or E_F, which is the threshold of the emission spectrum. The insets in the figure show Zn 3*d* SPEM images (cross-sectional views) of the ZnO NC and NW. The bright areas in the SPEM image correspond to the regions of the ZnO NC and NW with the maximum Zn 3*d* intensity. The spectra were obtained in three selected areas A, B and C, which are marked in the insets of the images of the ZnO NC and NW. The low spatial resolution of SPEM makes it difficult to distinguish among the thick, thin and impurity/edge (non-stoichiometric) regions in the ZnO nanostructures. However, the general line shapes of the valence-band SPEM spectra of ZnO NC and NW are similar to those that have been obtained previously from aligned ZnO nanorods.[1,2] Clearly, Fig. **S1** indicates that the intensity of feature **I** in the SPEM spectra of ZnO NC is remarkably larger than that in the SPEM spectra of the NW. In contrast, the intensities of feature **II** are nearly the same for ZnO NC and NW. Since, the occupied states at/below E_{VBM} or E_F are dominated by defects (or dangling/unpaired bonds) and/or the anion-derived *p* states, which are the O 2*p*-derived states in the ZnO nanostructures, the strong enhancement of feature **I** in the ZnO NC is attributed to the higher density of O 2*p*-derived states. On the other hand, feature **II** is deep in the valence band, can be attributed to the O 2*p* and Zn 3*d*/4*sp* hybridized states.[1,2]

The results of O *K*-edge STXM-XANES (probing the local DOS at/above E_{CBM} or E_F) and valence-band SPEM measurements (probing the local DOS at/below E_{VBM} or E_F) together strongly support the fact that the higher d^0 ferromagnetism in ZnO NC in comparison with the NW is closely related to the enhancement of the O 2*p*-derived states near/at E_F. Further, it supports that these enhancement of the O 2*p*-derived states near/at E_F is strongly depends on concentration of defects/vacancies at O sites in the impurity/edge (non-stoichiometric) region, which is higher in ZnO NC compare to NW.

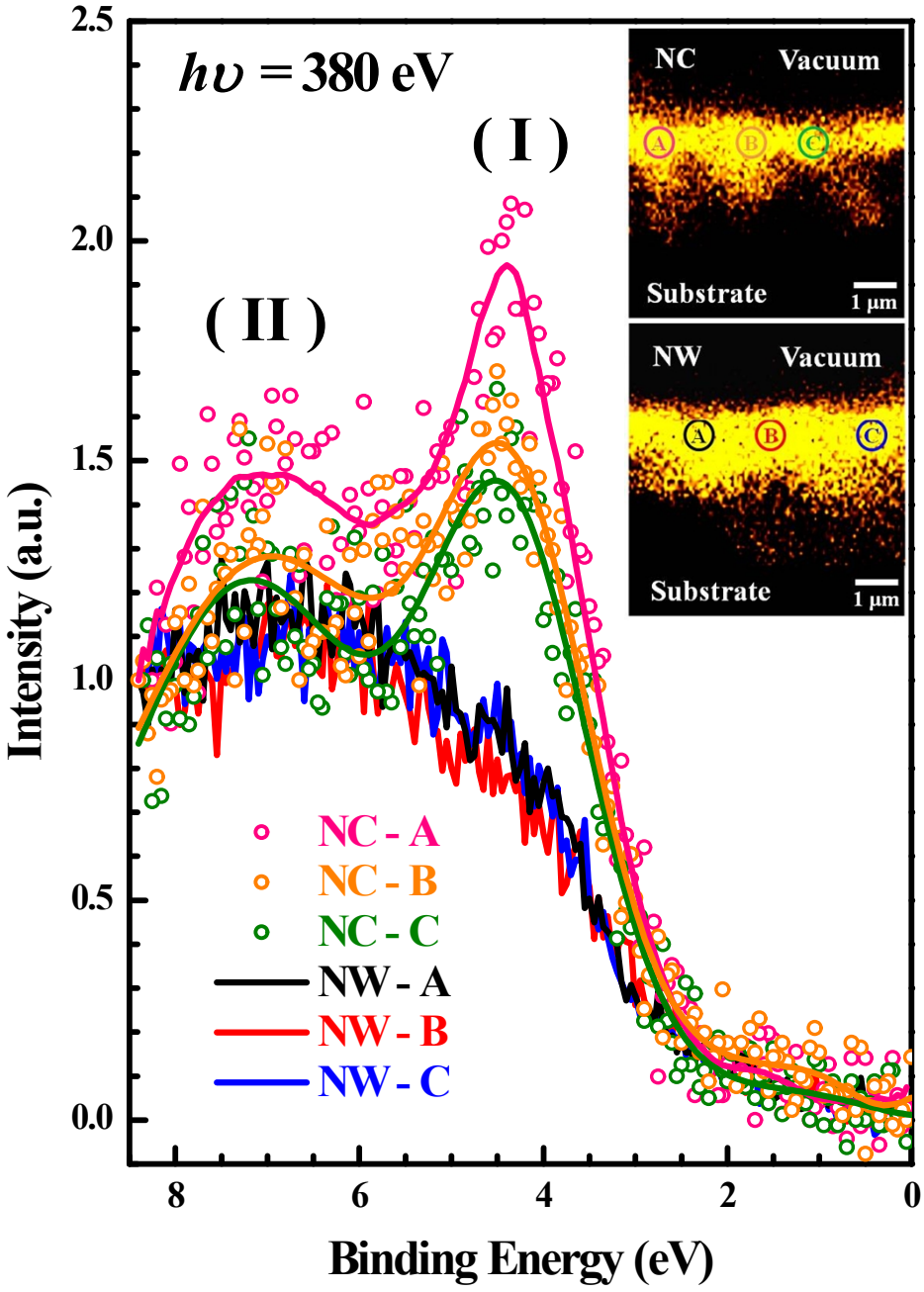

Figure S1 (color online) Displays spatially resolved valence-band SPEM spectra of the ZnO NC and NW, obtained from three selected areas (A, B and C). The solid lines that smoothly fit the SPEM spectra of the ZnO NC were guided by eye. Inset shows Zn 3*d* SPEM images of cross-sectional views of ZnO NC and NW, respectively.

Computational details: In this work, the ground-state electronic and magnetic structures of bulk wurtzite ZnO with various neutral vacancy defects were calculated by means of the first-principles full-potential projector augmented wave (PAW) method[3], which was implemented in the Vienna *ab initio* simulation package (VASP) package[4]. The calculations were based on density functional theory (DFT)[5], which incorporates exchange and correlation functionals in a local density approximation (LDA)[6]. Since, the under-binding of the *d*-orbital of Zn in the LDA, which overestimates *pd* hybridization and significantly underestimates the band gap in bulk ZnO, a rotationally invariant LDA+U method[7] was used, with a screened Coulomb potential and exchange parameters (U= 8.0 eV and J= 0.95 eV)[8] that were calculated from first principles. To study the defect-induced spontaneous spin polarization, the calculations were performed for neutral native vacancies in 72-atom wurtzite supercells. A cutoff energy of 750 eV for the basis set was used, and a 6x6x3 Monkhorst-Pack *k*-grid sampling[9] was carried out to obtain the Brillouin-zone integrals to ensure convergence.

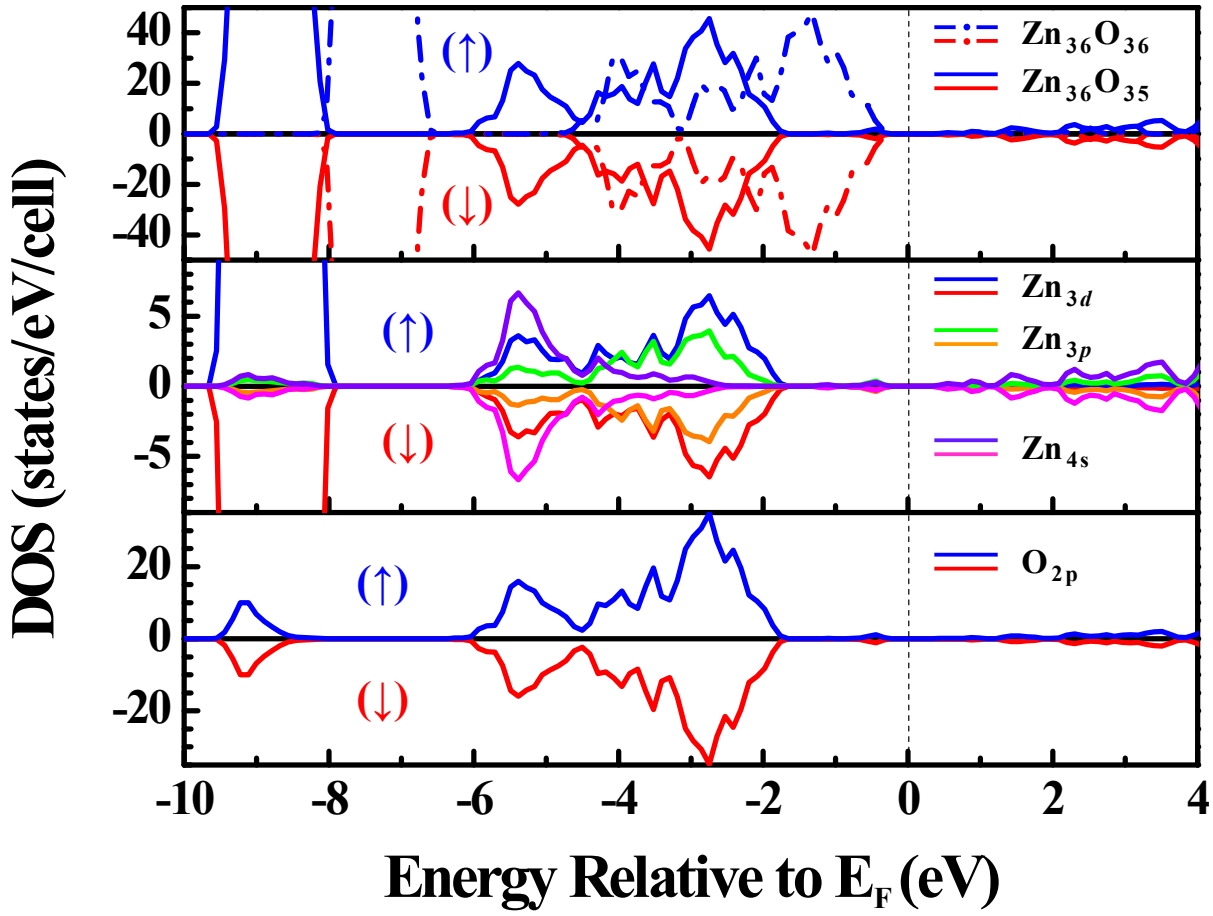

FIG. S2: Calculated total electronic density of states (TDOS, in top panel) and partial density of states (PDOS) of Zn 3*d*, Zn 3*p* and Zn 4*s* (middle panel) and O 2*p* (bottom panel) of bulk wurtzite ZnO with oxygen anion vacancies (V_O) ($Zn_{36}O_{35}$, indicated by solid lines). TDOS of defect-free bulk ZnO ($Zn_{36}O_{36}$, indicated by dotted lines) is also presented in top panel for comparison. E_F (denoted as a dashed line) is aligned to 0 eV. Notably, V_O in $Zn_{36}O_{35}$ does not contribute to any local net spin moment.

Stoner model:[10,11] In this model, ferromagnetic structure appears when the electronic structure satisfies the *Stoner criterion*: $ID(E_F) > 1$, where I is the Stoner parameter, and $D(E_F)$ is the DOS at E_F. The Stoner parameter I, which is a measure of the strength of the exchange interaction, can be determined from the total energy difference between the nonmagnetic (non-spin-polarized LDA+U) and ferromagnetic (spin-polarized LSDA+U) calculations. In our case, the Stoner parameters I of V_{Zn} and V_O are 0.22 eV and 0 eV, respectively, which are in agreement with early theoretical work.[12] To predict the onset of vacancy-induced ferromagnetism, the spin-polarization effects on the TDOS were also examined by comparing the nonmagnetic (LDA+U, black curve in Fig. S3) and ferromagnetic (LSDA+U, blue and red curves in Fig. S3) calculations. In fact, the significant $D(E_F)$ of 17.3 was obtained from the LDA+U calculation, when combined with a non-negligible I, indicates that ZnO with a V_{Zn} defect meets the *Stoner criterion* and favors the presence of a ferromagnetic phase.

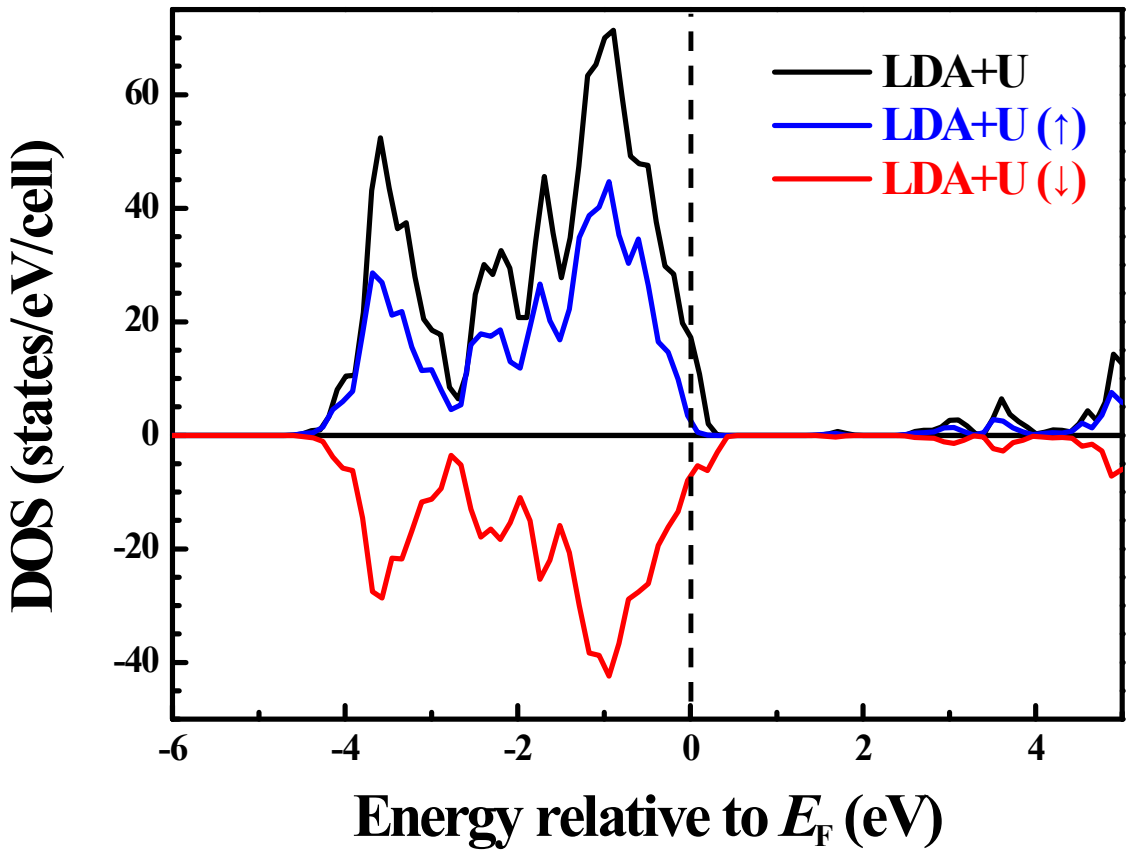

Fig. S3 TDOS obtained from nonmagnetic (LDA+U, black curve) and ferromagnetic (LSDA+U, blue and red curves) calculations, respectively. E_F denoted as the dashed line is aligned to 0 eV.

References

1. J. W. Chiou, J. C. Jan, H. M. Tsai, C. W. Bao, W. F. Pong, M. H. Tsai, I. H. Hong, R. Klauser, J. F. Lee, J. J. Wu *et al.*, *Appl. Phys. Lett.* **2004**, 84, 3462-3464.

2. J. W. Chiou, K. P. K. Kumar, J. C. Jan, H. M. Tsai, C. W. Bao, W. F. Pong, F. Z. Chien, M. H. Tsai, I. H. Hong, R. Klauser, R. *et al., Appl. Phys. Lett.* **2004,** 85, 3220-3222.

3. P. E. Blöchl, *Phys. Rev. B* **1994**, 50, 17953-17979.

4. G. Kresse and J. Hafner, *Phys. Rev. B* **1993**, 47, 558-561.

5. P. Hohenberg and W. Kohn *Phys. Rev.* **1964**, 136, B864-B871.

6. W. Kohn and L. J. Sham, *Phys. Rev.* **1965**, 140, A1133-A1138.

7. S. L. Dudarev, G. A. Botton, S. Y. Savrasov, C. J. Humphreys and A. P. Sutton, *Phys. Rev. B* **1998**, 57, 1505-1509.

8. B. C. Shih, Y. Xue, P. Zhang, M. L. Cohen and S. G. Louie, *Phys. Rev. Lett*. **2010**, 105, 146401.

9. H. J. Monkhorst and J. D. Pack, *Phys. Rev. B* **1976**, 13, 5188-5192.

10. E. C. Stoner, *Proc. R. Soc. Lond. A* **1938**, 165, 372-414.

11. E. C. Stoner, *Proc. R. Soc. Lond. A* **1938**, 169, 339-371.

12. H. K. Chandra and P. Mahadevan, *Solid States Commun*. **2012**, 152, 762-766.